IDRC 2025 NICOSIA | 8th International Disaster and Risk Conference

Disaster evacuation of the old city of Nicosia

Marios Stylianou[a,*], Marios Demetriou[a,**] and Andreas Aristidou[a,b]

[a] University of Cyprus, Department of Computer Science, Nicosia, 1678, Cyprus
[b] CYENS Centre of Excellence, Nicosia, 1016, Cyprus

ARTICLE INFO

Keywords:
Crowd simulation
Vehicle evacuation
Urban areas
Disaster evacuation

ABSTRACT

Historic urban centers face unique evacuation challenges due to their dense morphology, aging infrastructure, and cultural preservation constraints. This study focuses on Nicosia's walled Old Town, a complex environment shaped by 16th-century fortifications, irregular street patterns, and limited access through six operational gates. Using a high-fidelity, geo-referenced digital twin of the area, we simulate evacuation scenarios under various stress conditions, including road closures, gate blockages, and alternative shelter placements, through a hybrid agent-based model built in Unity. Our findings reveal that certain conditions lead to significant evacuation delays, and that uncoordinated infrastructure additions may worsen outcomes without proper guidance mechanisms. This work highlights the importance of coupling infrastructure upgrades with adaptive flow-management strategies and provides an open-source dataset to support future research in disaster risk reduction and crowd dynamics in historic cities.

1. Introduction

Historic city centers represent a complex intersection of cultural heritage preservation and urban vulnerability. This tension is particularly evident in Nicosia, Cyprus, where the Old Town, enclosed by 16th-century Venetian fortifications and structured around an irregular street network, presents significant challenges for emergency evacuation. The walled city, partially bordered by a military buffer zone, retains only six operational gates and is characterized by a dense pattern of narrow, pedestrian, and one-way streets. These constraints not only impede everyday mobility but also critically hinder the ability to conduct safe and timely evacuations during disasters.

In recent years, the Eastern Mediterranean has faced a growing number of climate-related and human-induced disasters, highlighting the urgent need for evidence-based disaster risk reduction (DRR) strategies in historic urban centers. Although Nicosia participates in the UNDRR Making Cities Resilient 2030 program, its emergency master plan remains schematic and lacks a detailed, data-driven evacuation model that captures the interaction of pedestrian and vehicular flows at city scale. Prior studies on Mediterranean heritage cities often focus on single hazards, use simplified networks, or overlook the effects of political boundaries (Arrighi et al., 2023), leaving a critical gap in understanding how multi-hazard exposure, historic morphology, and real-time decision-making intersect in vulnerable contexts.

To address this, we employ a high-fidelity 3D digital twin of Nicosia's Old Town[1]. This model supports realistic visualization and simulation of evacuation scenarios, helping identify hidden vulnerabilities and potential bottlenecks. We integrate a hybrid agent-based model using Unity's AI Navigation system augmented with custom behavioral logic, calibrated through traffic counts and crowd-density surveys. The simulation environment includes terrain meshes, semantic road layers, and parameterized hazard zones in a fully geo-referenced, open-source digital replica of the Old Town.

In this work, we conducted a series of dynamic test scenarios under various stress conditions, such as road closures, gate blockages, and alternative shelter placements. By integrating physically realistic agent behavior with accurate topographical data, we produced actionable insights for urban planners, emergency services, and policy-makers. Our simulation experiments reveal that evacuating Nicosia's semicircular walled core can become significantly delayed under certain conditions, and that adding infrastructure, without first providing clear guidance to residents, fails to improve evacuation outcomes. The resulting simulation dataset offers a valuable foundation for future academic research in crowd dynamics and evacuation modeling. This work makes the following contributions:

- Enhanced the high-fidelity digital twin of Nicosia's Old Town by integrating geographic road network data and a hybrid agent-based model to enable real-time evacuation scenario testing and stakeholder engagement.
- We present a hybrid agent-based simulation framework that models pedestrian and vehicle dynamics

*Corresponding author. Email: stylianoumarios@outlook.com
**M. Stylianou and M. Demetriou contributed equally to this work.
stylianoumarios@outlook.com (M. Stylianou); demetrioumarios87@gmail.com (M. Demetriou); a.aristidou@ieee.org (A. Aristidou)
ORCID(s): 0000-0001-7754-0791 (A. Aristidou)

[1] https://inicosia.cyens.org.cy/

using Unity's AI Navigation system, enhanced with custom behavioral logic.

- We conduct a series of evacuation experiments to evaluate system performance under stress, quantifying clearance times, congestion hotspots, and shelter saturation effects.

Our results also underscore the need to complement physical infrastructure upgrades with adaptive, real-time flow-management strategies. These can be effectively developed and tested using high-fidelity digital twins, which offer a robust platform for evaluating alternative exit layouts, routing protocols, and shelter-allocation policies before any on-site implementation. All artifacts, including source code, agent behavior logs, and congestion heatmaps, will be released as an open dataset to support continued research in urban resilience.

2. Related Work

Evacuation planning in dense, historic urban environments presents distinct challenges that transcend conventional transportation and civil engineering paradigms. In particular, the irregular morphology, restricted egress points, and mixed traffic patterns characteristic of heritage city centers demand a multidisciplinary approach.

In general, agent-based frameworks such as those presented in Pelechano et al. (2007) and Kapadia et al. (2013) have significantly advanced the realism of crowd movement by integrating psychological and perceptual models. These systems support dynamic obstacle avoidance, group behavior, and real-time replanning, key capabilities when simulating evacuation through constrained, evolving spaces. Narain et al. (2009) and Karamouzas et al. (2014) introduced data-driven and velocity-based crowd models, respectively, enabling smoother, more predictive simulations that scale efficiently to dense urban populations.

In terms of city evacuations scenarios, early contributions to pedestrian dynamics include the work of Helbing et al. (2000), who introduced the Social Force Model (SFM), a continuous micro-simulation framework that has since been widely adapted for emergency scenarios. Extensions of this model by Yang et al. (2022) introduced behavioral heuristics, including panic escalation and adaptive exit selection, to better reflect decision-making in disaster contexts. Bernardini et al. (2021) further coupled pedestrian exit models with flood simulations, demonstrating that historical morphologies can produce localized deviations in evacuation times exceeding 15%. Finally, works like Hassanpour and Rassafi (2021) presents an agent-based simulation model that incorporates the concept of affordance to analyze pedestrian evacuation behavior during emergencies.

Multi-modal evacuation, where both pedestrian and vehicular flows must be considered, introduces additional complexity. Zhang and Chang (2014) proposed a dynamic network flow model that jointly optimizes evacuation routes while resolving pedestrian-vehicle conflicts at intersections. Ronchi and Nilsson (2013) integrated vehicle dynamics into the FDS+Evac environment, revealing that spontaneous mode-switching behaviors (e.g., abandoning vehicles mid-evacuation) can have major implications for system-wide throughput. Additional work by van den Berg et al. (2008) in reciprocal collision avoidance has informed many graphics-based simulations where pedestrians and vehicles share space under time pressure.

The growing maturity of digital twin technologies has opened new possibilities for urban DRR. Frameworks such as Batty (2024) and Therias and Rafiee (2023) highlight the role of 3D urban models and sensor feedback in resilience planning. From a participatory planning perspective, Wang et al. (2024) integrates GIS data with public engagement tools, though few models achieve centimeter-scale resolution or simulate full-scale evacuations. Notably, graphics platforms like Unity and Unreal Engine have been adapted to support high-fidelity, agent-based urban simulation, as demonstrated in Guy et al. (2009) and Kallmann and Kapadia (2014), offering both visual realism and behavioral plausibility.

Our work builds on these foundations by integrating high-resolution spatial data, scenarios with pedestrian and vehicle simulations, and behavioral calibration into a real-time, interactive digital twin of Nicosia's Old Town. This allows for the testing of multi-hazard evacuation scenarios under realistic constraints, such as blocked gates or roads, narrow corridors, etc. providing actionable insights for heritage city DRR planning.

3. Methodology

This section outlines the development and implementation of our simulation framework. We describe the 3D environment setup, network reconstruction, shelter modeling, agent behavior design, and traffic dynamics.

3.1. Simulation Environment

All simulations were developed in *Unity*, which offers an integrated 3-D renderer, physics solver, and AI navigation toolkit. The digital twin of Nicosia's Old Town, taken from i-Nicosia, was imported as textured meshes, providing georeferenced buildings, terrain, and infrastructure elements such as walls and street furniture. This model forms the spatial foundation for evacuation scenario testing.

3.2. Network Reconstruction and Nav. Layer

The road network was reconstructed using *EasyRoads3D*, manually aligning each segment with the twin geometry to preserve geometric accuracy. The six historic gates were defined as the only legal exit points, reflecting the constraints imposed by the 16th-century fortifications. Due to the military buffer zone in the north, vehicles and pedestrians are restricted from crossing that boundary (as seen in Figure 1).

To enforce one-way street constraints and prevent unrealistic routing, we used Unity's AI Navigation system to build a detailed *navigation mesh* (nav-mesh), overlaid with

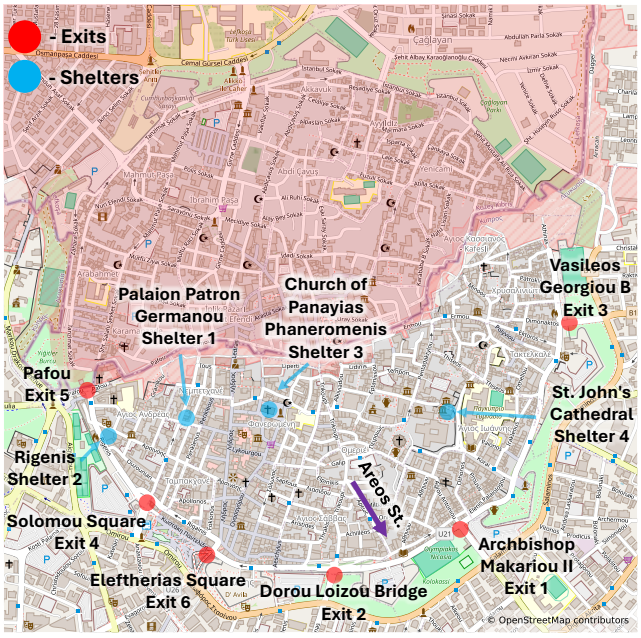

Figure 1: Geo-referenced 3D map of Nicosia's Old Town, showing city gates (exits), active shelters, and the military buffer zone to the north.

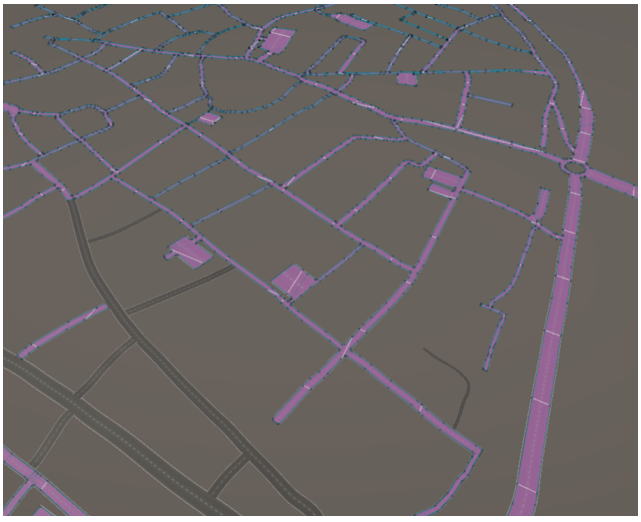

Figure 2: Navigation mesh overlaid on reconstructed road geometry, including one-way links and walkable/driveable surfaces.

directional off-mesh links that encode one-way restrictions. Note that, pedestrian-only paths were excluded from the vehicle navigation layer. The resulting multi-layered nav-mesh is shown in Figure 2.

3.3. Shelter Modeling

Shelters were represented as dynamic nodes within the simulation. Consultation with Cyprus Civil Defense confirmed two active shelters (with capacities of 180 and 200), and two additional sites pending activation. Each shelter was parameterized with its capacity, and agents were programmed to select the nearest shelter but redirect dynamically if capacity was exceeded. This redirection logic allowed for realistic modeling of queuing, spillover flows, and localized congestion effects.

3.4. Agent Modeling

To simulate realistic evacuation behavior, we modeled two main agent types: pedestrians and vehicles. Each type is governed by distinct motion dynamics, perception rules, and decision-making processes. Both agent systems operate in the same navigable environment but respond differently to congestion, routing, and environmental cues.

3.4.1. Pedestrians

Pedestrian agents used Unity's nav-mesh for global path planning and a lightweight motion controller for local steering and skeletal animation. Parameters such as acceleration, avoidance radii, and stopping distance were manually calibrated to mimic real-world walking dynamics. To model varied familiarity with the city layout, and represent heterogeneous knowledge, we implemented a leader–follower mechanism: these agents follow a designated leader until nearing a gate or shelter, then switched to individual pathfinding. This behavior generated emergent platoon dynamics, similar to tourist or group evacuation behavior.

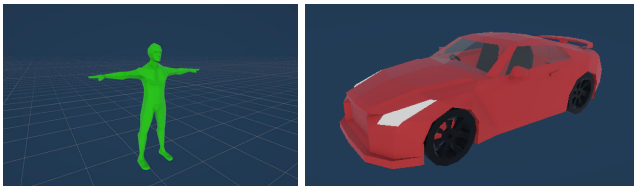

Figure 3: Agent models used in the simulation. Human agents use Unity's Animator for skeletal motion (pedestrian prefab on the left); vehicles employ rigid-body dynamics (vehicle prefab on the right).

3.4.2. Vehicles

Vehicle behavior posed unique challenges. Unity's default nav-agent was initially adapted for cars, but this yielded unrealistic motion. Instead, we developed a custom *CarController* script. Each vehicle still used the nav-agent path for navigation, but actual motion was computed by applying physical forces and torques to a rigid body, producing more lifelike acceleration, deceleration, and turning. To avoid collisions, we combined Unity's Reciprocal Velocity Obstacles (RVO) module with three front-facing ray-casts (Figure 4), which detect obstructions and modulate throttle in real time.

Navigation decisions were made using a "fewest-corners" heuristic rather than Euclidean distance, reflecting the complexity of one-way grids. After running a number of simulations, we observed that strictly following these precomputed routes created unrealistic behavior, as real drivers will often detour when they spot heavy traffic. To model real-time driver adaptation, we implemented congestion triggers: each

Figure 4: A snapshot of vehicle simulation within a 3D model of Nicosia. A ray-cast system enables vehicle collision avoidance by detecting frontal obstacles and adjusting throttle accordingly.

street segment monitored its vehicle density and, if overloaded, increased its nav-mesh cost. Therefore, all streets have their own Navmesh area and a congestion threshold customized to its width and position. Approximately 25% of agents responded by recalculating their route, producing a plausible mix of compliant and opportunistic drivers.

3.5. Speed Calibration

Pedestrian agents were assigned walking speeds from a normal distribution $\mathcal{N}(\mu = 8 \text{ km/h}, \sigma = 1.5)$, ensuring diversity in crowd dynamics. This distribution was selected based on publicly available data on average adult running speeds over short distances (≤ 600 m), which corresponds to the mean evacuation distance required for agents to reach nearby exits. Vehicle agents were assigned a maximum velocity of 30 km/h, consistent with the speed limit within the Old City boundaries, with modest tail-end overruns permitted on uninterrupted segments to reflect realistic driving variability. These parameter choices were validated through repeated simulation trials to ensure consistency with observed pedestrian and vehicular behaviors.

4. Results

4.1. Implementation Details

Our simulation was implemented in Unity 6 Preview (version 6000.0.19f1, DX11), using the Unity AI Navigation package (version 2.0.4) for pathfinding and EasyRoads3D Free v3 (version 3.2.4f3) to generate an accurate road network.

4.2. Experimental Scenarios

This section presents the research hypotheses (H_A and H_B) along with the evacuation scenarios designed to test them. Each scenario is designed to serve a dual purpose: (i) to evaluate the hypotheses, and (ii) to assess the robustness of the simulation framework by identifying potential limitations or sources of error. Collectively, these experiments provide a systematic evaluation of the old town's road network under stress, offering insight into its capacity to support rapid evacuations and overall urban resilience during critical events.

All scenarios were executed within fixed simulation time limits, 10 minutes for pedestrian-only trials and 15 minutes for vehicle runs, to enable consistent comparison across conditions. The baseline population includes 3000 pedestrian agents and 700 vehicles, representing peak activity within the city walls, encompassing residents, workers, and visitors. The city population was determined based on demographic data reported in the *Census of Population and Housing 2021*, conducted by CYSTAT (2024). To reflect varying levels of route familiarity, scenarios were repeated with different leader-to-follower ratios: leaders know how to navigate, while followers relied on nearby leaders for guidance, simulating individuals unfamiliar with the local escape routes. Agents were initialized on the road network and remained stationary until the evacuation signal was issued. The model assumes a closed system, with no additional entries into the simulation area during the event.

4.3. H_A: Limited Clearance Without Shelters

This hypothesis investigates whether the old town can be fully evacuated, on foot or by car, within a reasonable time frame when no shelters are available. We designed two scenario suites to assess pedestrian and vehicle evacuation independently. The pedestrian suite comprises five runs, each with a different leader-to-follower ratio: 80:20, 60:40, 40:60, 20:80, and an intermediate 50:50 split. Results are averaged across these five runs. The vehicle suite consists of five identical runs, and their outcomes are likewise averaged to obtain representative performance metrics.

4.3.1. Pedestrian Evacuation Scenarios

Two pedestrian-focused scenarios were evaluated to assess evacuation performance and the city's ability to support foot traffic during critical events.

Pilot Scenario: All six exit points were made available to establish benchmark performance without shelters. As shown in Figure 5a, most agents traveled between 100–400 m (blue bars), with corresponding evacuation durations clustering between 100–200 s in Figure 5b. Evacuation success varied by agent type: leaders performed well, with a 95.7% completion rate within the 10-minute window. In contrast, many followers failed to evacuate due to loss of contact with their guides. The "Dorou Loizou Bridge" emerged as the most frequently used exit, suggesting strong spatial preference that may inform future gate-specific traffic policies.

Critical Exit Blockage Scenario: Here, we disabled the "Dorou Loizou Bridge", the most preferred exit, to test the system's adaptability under constrained conditions. The leaders' success rate decreased to 90%, while follower performance remained similar. Figures 5a and 5b (red bars) show broadened distributions in both travel distance and

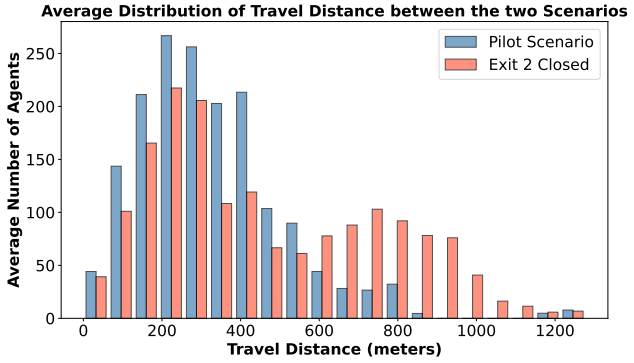

(a) Distribution of Travel Distances Among Agents.

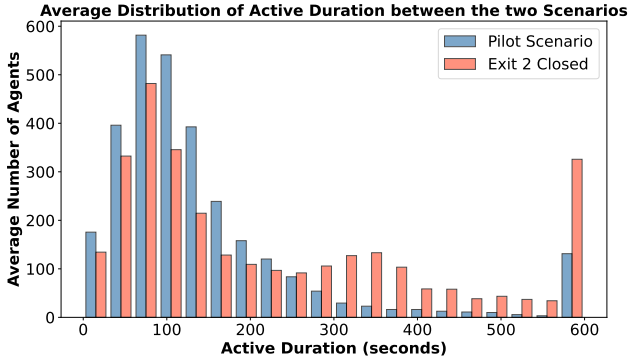

(b) Distribution of Active Duration Among Agents.

Figure 5: Histogram comparison between pilot and critical exit blockage scenarios regarding travel distance and active duration with average number of agents across five runs.

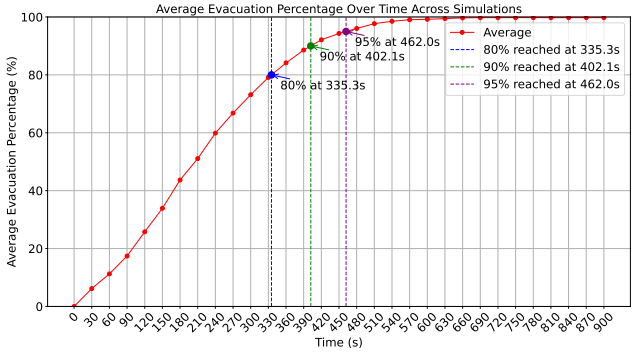

Figure 6: Cumulative percentage of vehicles evacuated over time in the pilot scenario.

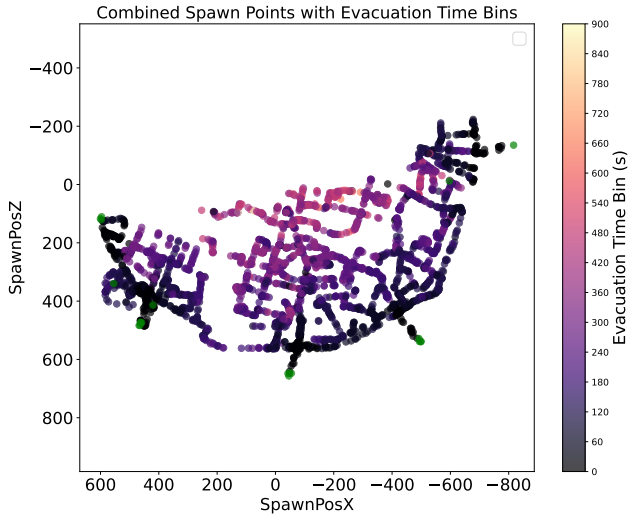

Figure 7: Vehicle spawn locations color-coded by evacuation time. Darker colors indicate faster clearance.

evacuation time. Agents initially moved toward the blocked exit, rerouting only upon arrival, resulting in detours and delays. "Plateia Eleutherias" exits absorbed most of the rerouted flow, becoming the new bottleneck.

4.3.2. Vehicle Evacuation

We next evaluated vehicle-based evacuations through two core scenarios, a pilot trial and a set of targeted disruptions.

Pilot Scenario: All exits were open. As shown in Figure 6, 80% of vehicles exited within 5.5 minutes (335.3 s), with 95% clearance achieved by 11.5 minutes. Exit usage analysis reveals that 76.1% of vehicles used central and eastern gates, primarily "Archbishop Makariou II" and "Dorou Loizou Bridge", while only 23.9% exited westward. This skew underscores the critical role of central arteries and highlights the vulnerability of the western sector, which depends on a single arterial connection serving "Solomou Square" and "Pafou" exits. Spatial evacuation patterns are shown in Figure 7, where vehicle spawn points are color-coded by evacuation time. As expected, vehicles originating from the city center or northern blocks took significantly longer to exit compared to those positioned near the periphery.

Figure 8 presents the average congestion levels during evacuation. High-traffic zones are denoted by brighter cells, corresponding to bottlenecks and high-demand segments. A few anomalies (circled in red) may be attributed to data noise or clustering artifacts. The main streets with consistently high congestion are: Areos Str, Achileos Str, Athinon Str, Onisilou Str, Xatzigeorgaki Kornesiou Str, and Patriarchou Grigoriou Str.

Exit and Road Blockage Scenarios: To evaluate the network's resilience, we conducted a series of sub-scenarios in which major exits or critical road segments were selectively blocked. Performance was assessed using the same metrics as in the pilot. Among the seven sub-scenarios, two blockages had notable effects. When the "Archbishop Makariou II" exit was disabled, the overall evacuation rate remained high but fell short of full clearance within 15 minutes, highlighting the critical role of this central road. Similarly, the closure of "Areos" Street (see Figure 1), a key one-way connector, left approximately 1–2% of vehicles stranded within the city.

Conversely, when the "Areos" feeder to "Dorou Loizou Bridge" was blocked, most vehicles rerouted efficiently to

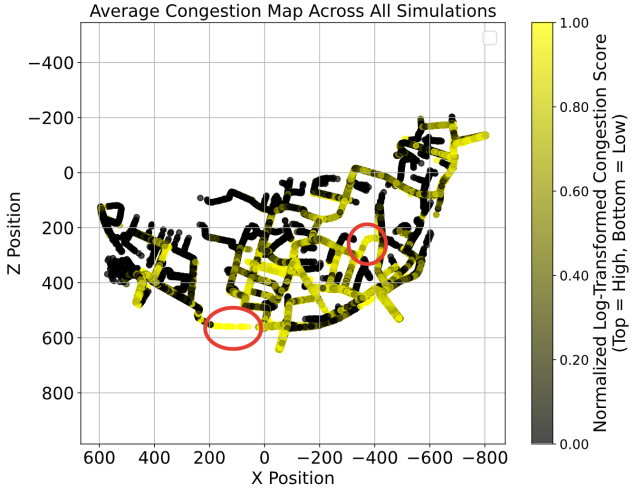

Figure 8: Average vehicle congestion map during pilot evacuation. Brighter areas indicate higher traffic density.

the "Archbishop Makariou II" and "Vasileos Georgiou B" exits. Although clearance times increased slightly, evacuation remained largely successful, demonstrating the network's adaptive potential under moderate stress.

4.4. H_B: Shelter Capacity and Distribution

The second hypothesis evaluates whether the existing shelter system, both in overall capacity and spatial placement, is sufficient to protect the old town population in a timely manner. We posit that the current pair of operational shelters cannot accommodate most occupants within an acceptable interval. To test this, we conducted two pedestrian-only scenarios, each with 3000 agents, and compared their outcomes. As before, the pedestrian suite includes five runs, with different leader to follower ration, with results averaged across them.

Pilot Scenario (2 Shelters): All six exit gates were open and the two operational shelters were enabled. Figure 9a (blue bars) shows that the majority of agents walked less than 300 m to reach either a gate or a shelter. Correspondingly, evacuation times in Figure 9b (blue bars) peak sharply below 100 s and decline steadily thereafter. This long-tail distribution confirms that proximity to a shelter is the primary determinant of clearance time, whereas agents spawned in poorly served areas must traverse nearly the entire network before reaching safety.

Expanded-Shelter Scenario (4 Shelters): The second scenario activated two additional, yet-to-be-commissioned shelters, increasing the total to four. This configuration isolates the effect of added capacity and more central placement on network performance. Enabling the extra shelters produced a distinctly bimodal pattern in both metrics. In Figure 9a (red bars), a pronounced peak appears below 200 m, indicating that many agents reached a new shelter almost immediately. A secondary rise near 1000 m reflects agents who still had to traverse the full network (mainly searching for a nearby shelter, before exiting the city). The evacuation-time histogram in Figure 9b (red bars) mirrors this split: a large share clears in under 100 s, while another cohort exceeds 300 s (≈ 5 min). These results highlight spatial heterogeneity: centrally located shelters dramatically reduce clearance times for nearby occupants, yet peripheral zones remain underserved.

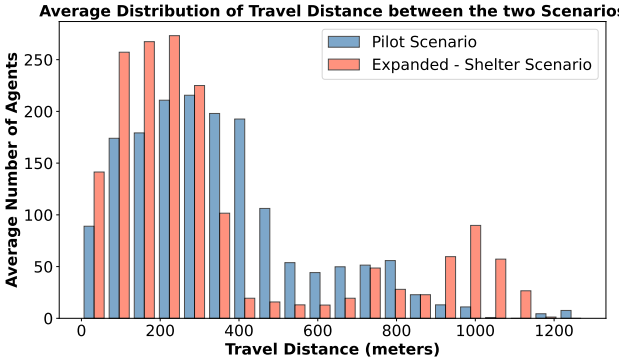

(a) Travel-distance distribution for pilot (blue) and Expanded-Shelter (red) scenarios.

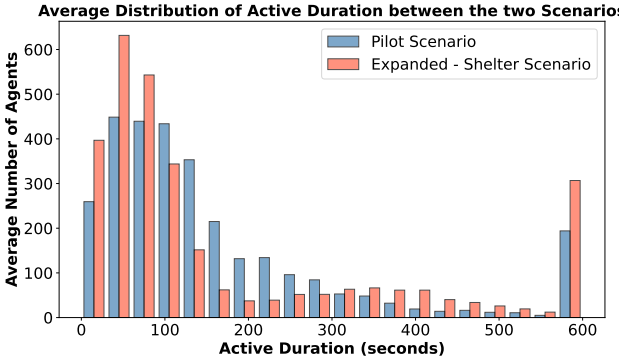

(b) Evacuation-time distribution for pilot (blue) and Expanded-Shelter (red) scenarios.

Figure 9: Effect of additional shelters on pedestrian evacuation performance.

5. Discussion

This section analyzes the results of each set of scenarios, highlighting how evacuation times and success rates change under different network and shelter configurations, as introduced in Hypotheses H_A and H_B. Finally, we reflect on the extent to which our simulations reproduce plausible crowd and traffic dynamics during emergencies, drawing implications for the resilience of the walled center of Nicosia and for future mitigation measures.

5.1. Impact of Network Disruptions (H_A)

5.1.1. Pedestrian Scenarios

Figure 10a shows the cumulative share of *leader* agents reaching safety over time, averaged across runs with varying leader-to-follower ratios. The pilot (blue curve), with all six gates open, clears significantly faster than the exit-blocked scenario (red curve). At the 50% threshold, leaders evacuate

on average 39 seconds earlier in the pilot; this gap widens to 190 seconds at 80% and 320 seconds at 90%, revealing a nonlinear decline in efficiency when the key gate is closed.

Figure 10b shows a similar trend for follower agents but with lower success rates. Many followers lose visual contact with their leader during congestion and are removed from the simulation, causing an early plateau in clearance rates. This underscores the fragility of leader-dependent evacuation.

Histograms of travel distance (Figure 5a) and active duration (Figure 5b) reveal long-tailed distributions: some agents must walk 700–1000 meters and take 300–400 seconds to reach safety. Blocking the popular "Dorou Loizou Bridge" shifts nearly all displaced traffic to the "Plateia Eleutherias" exit, creating a new congestion hotspot.

Another important observation arises when analyzing different leader-to-follower ratios. Leader agents consistently achieve high success across all scenarios, showing they can navigate effectively even when key exits are blocked. Their evacuation times remain fast and stable regardless of the population composition. However, follower agents are heavily dependent on leader presence. When leaders form the majority ($\geq 70\%$), clearance times decrease significantly, and almost all agents reach safety. In contrast, when leaders are made up of only 20%–50%, most followers fail to evacuate, resulting in low success rates and erratic evacuation times. A tipping point is observed around the 70% leader mark, beyond which followers begin to evacuate more quickly and reliably. As the proportion of leaders drops, disorientation among followers increases, leading to slower evacuations, reduced coordination, and increased failure to reach exits. These results highlight the critical role that leader density plays in ensuring the speed and success of large-scale evacuations.

Key takeaway: maintaining the operability of every gate is critical. Even under idealized conditions, where all agents are already on the street grid at alarm onset, the impact of closing a key gate is substantial, significantly hindering clearance for both leaders and followers. Decision-makers must take proactive measures and effectively inform the public about the evacuation plan, while also being prepared to issue clear guidance and implement real-time adaptive flow management to prevent secondary bottlenecks.

5.1.2. Vehicle Scenarios

Figure 11 shows the cumulative evacuation percentage over time, averaged across five identical runs. The pilot (blue) achieves full clearance within 15 minutes, while the closure of "Archbishop Makariou II" (red) delays the curve and prevents complete evacuation within the time window. The 80%, 90%, and 95% thresholds are reached roughly three minutes later on average, indicating significant delays and rerouting toward more distant exits. This traffic shift is evident in Figure 12, where red circles mark redirected flows toward "Dorou Loizou Bridge", and heavy congestion forms near "Vasileos Georgiou B", in contrast to the pilot.

In contrast, blocking "Areos" Street (Figure 13) produces only modest delays, shown in blue (pilot) and red (closure).

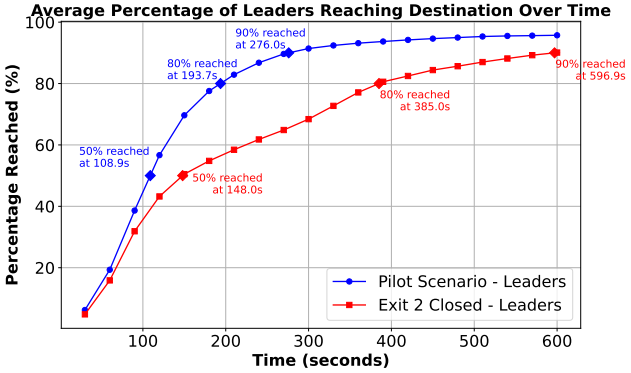

(a) Leaders: cumulative success over time (Pilot: blue; Exit blocked: red).

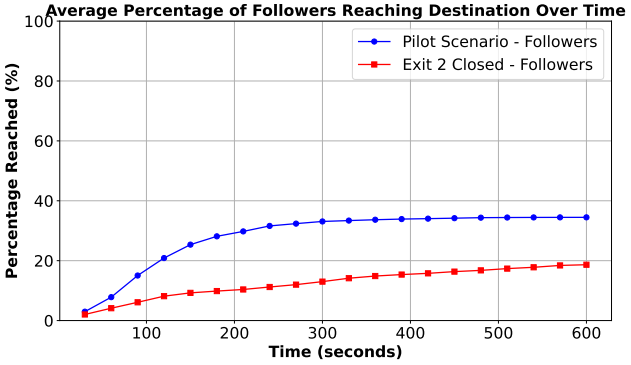

(b) Followers: cumulative success over time (Pilot: blue; Exit blocked: red).

Figure 10: Effect of disabling the *Dorou Loizou Bridge* gate on pedestrian evacuation.

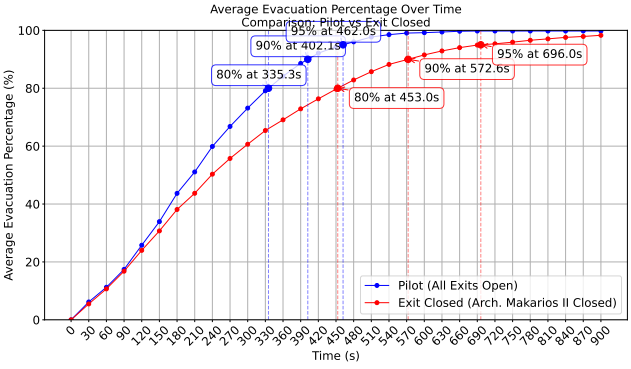

Figure 11: Exit Closure - Evacuation Percentage Comparison

Interestingly, the red curve briefly surpasses the pilot in the first minute, likely due to more focused routing toward direct exits. This early gain fades by minute five, as queuing on secondary streets offsets the initial advantage. Delays at the 80%, 90%, and 95% thresholds average around 55 seconds, far less than those caused by the exit closure of "Archbishop Makariou II". Note that, roughly 1–2% of vehicles remain

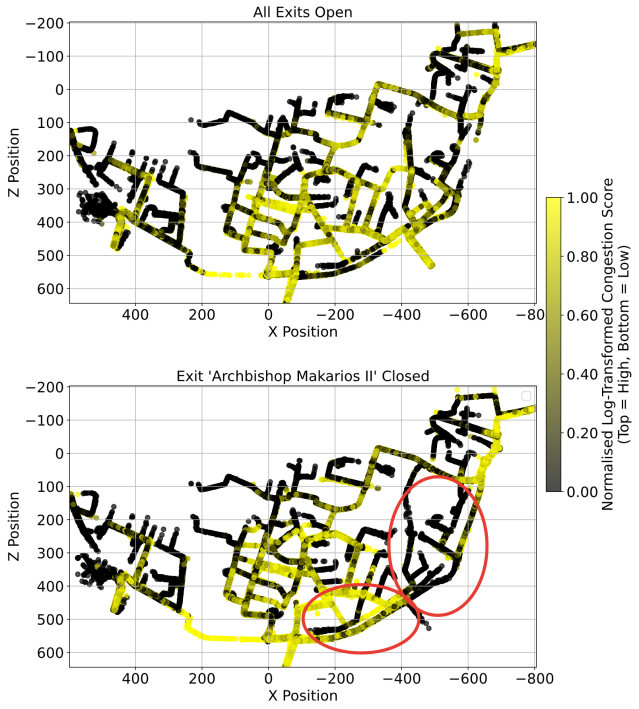

Figure 12: Congestion Graphs with all exits open(top) VS "Archbishop Makariou II" closed (bottom) where red circles highlight streets that congestion greatly changes.

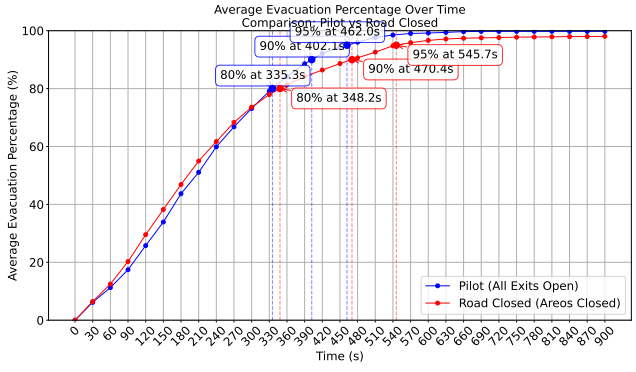

Figure 13: Road Closure - Evacuation Percentage Comparison.

trapped by one-way constraints. Figure 14 highlights the resulting spillover congestion (red circles) on adjacent streets, while the closure zone appears traffic-free (light blue).

Key takeaway: exit closures cause far more disruption than arterial road blocks. Keeping the exits open is critical to avoid gridlock and ensure timely evacuation. Decision-makers should prioritize the protection and accessibility of key exits in emergency planning, and implement adaptive flow management to prevent bottlenecks at alternate exits when blocked.Further details of all exit closures are provided in Table 1.

5.2. Shelter Capacity and Placement (H_B)

Figure 15a compares the cumulative evacuation of leader agents under two shelter configurations: the pilot with two

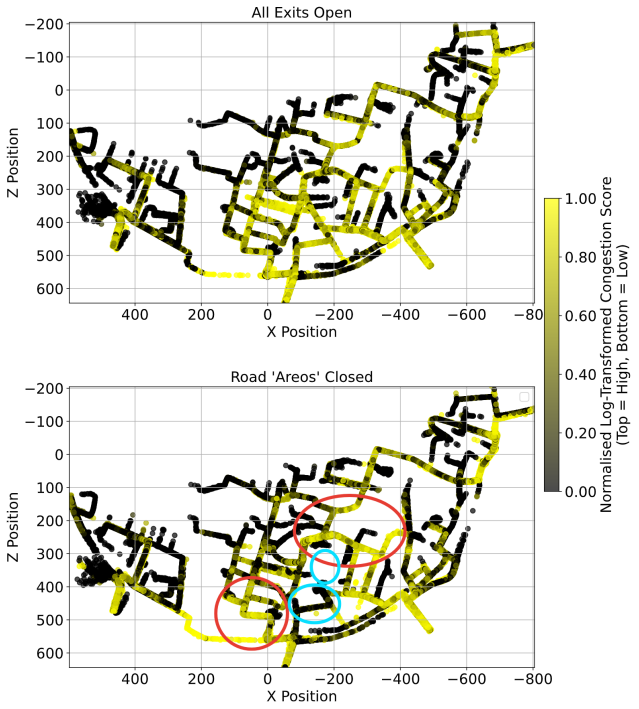

Figure 14: Congestion Graphs with all exits open (top) VS "Areos" Street closed (bottom). Red circles mark streets where congestion intensifies while the blue circles indicate the now traffic-free closed segment.

shelters (blue) and an expanded setup with four shelters (red). The added shelters offer a brief early advantage, e.g., 50% clearance is reached 28s sooner, but this reverses mid-run. The pilot surpasses the expanded setup, reaching the 80% mark 106s earlier and being the only one to hit 90% within the 10-minute window. This indicates that increasing shelter count without strategic placement or informing the public in advance about the most convenient location (shelter or exit), can hinder overall clearance.

Follower agents (Figure 15b) follow the same trend: initial gains under the four-shelter setup are lost midway, with the pilot ultimately achieving faster and more complete clearance. As in earlier scenarios, followers underperform leaders, reflecting their dependency and vulnerability.

Surprisingly, enabling two additional shelters did not uniformly improve clearance. The four-shelter configuration generates bimodal travel-distance and duration histograms (Figure 9). Although many pedestrians reach a shelter within 200m, a second peak near 1000m indicates that some were forced to visit multiple safe points after finding the nearest one full, extending their search and travel distance. Figure 16 shows this effect clearly: when Shelters 3 and 4 are added, traffic through Exits 1 and 2 is cut in half (shelters absorb much of the flow), and more people follow complex routes, from one shelter to another, or from a shelter to an exit. The Shelter Load Factor exceeded 1.2 in some facilities, indicating systemic overload. Post-hoc trace analysis revealed that nearly 18% of agents visited more than one shelter before successfully reaching safety, while some pedestrians

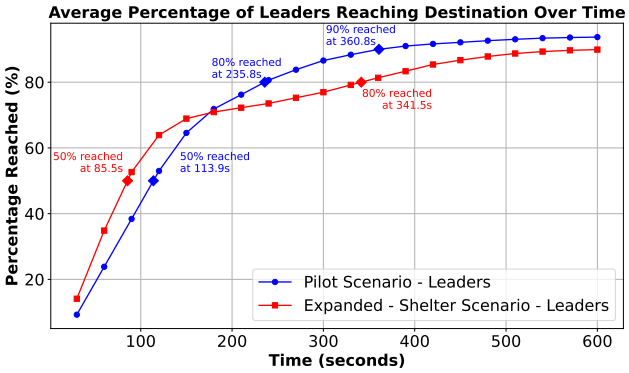

(a) Leaders: cumulative success (2 shelters: blue; 4 shelters: red).

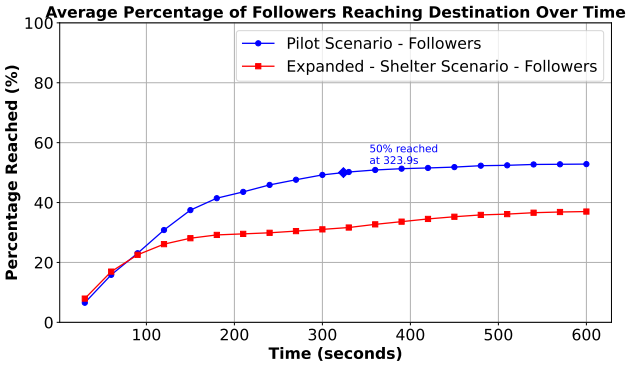

(b) Followers: cumulative success (2 shelters: blue; 4 shelters: red).

Figure 15: Impact of adding two centrally located shelters on pedestrian clearance.

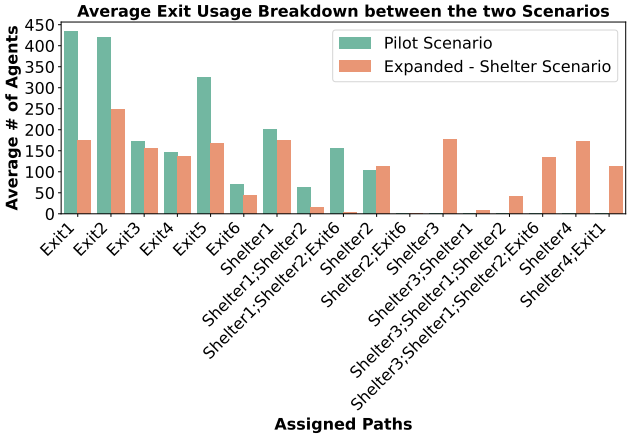

Figure 16: Gate and shelter usage in pilot with two Shelters (green) vs. Expanded Shelter(orange) configurations.

are rerouted up to three times, which explains the long delays seen in both distance and time.

Key takeaway: Simply adding shelter capacity does not guarantee faster evacuation or more people in safety. The findings confirm that the current shelter capacity is insufficient. However, adding shelters or other facilities indiscriminately, without dynamic guidance to under-used shelters, can trigger cascading reroutes and lengthen clearance times.

5.3. Implications for Risk-Informed Planning

The asymmetric congestion patterns and rerouting delays uncovered by the model underscore the need for adaptive evacuation strategies. Across both hypotheses, three strategic priorities emerge:

- Hardening key exit gates and ensuring their operability under duress. The loss of a single high-demand gate sharply degrades evacuation performance.
- Introducing dynamic signage or real-time guidance to alternative routes can prevent newly formed hotspots when primary routes fail.
- Additional capacity is effective only if pedestrians receive timely information that redirects them before a shelter reaches saturation.

Our results reveal that the walled Old Town of Nicosia has a fragile evacuation topology that is highly sensitive to gate availability and shelter distribution. Integrating redundant exit capacity, intelligent routing assistance, and shelter load-balancing could markedly improve clearance outcomes in real emergencies. Finally, the digital twin not only exposes latent vulnerabilities but also offers a rigorous platform for testing mitigation strategies.

5.4. Simulation vs. Protocols

To contextualize our simulation results, we compared them against existing disaster management frameworks, e.g., the Public Warning System (PWS), which underpins Cyprus's national evacuation and emergency response strategy. At the community level, the Polyvios Plan delegates responsibilities to local leaders or council-appointed individuals, who receive evacuation orders from Civil Defense authorities and disseminate alerts to residents via SMS, door-to-door notifications, church bells, sirens, or other audible signals.

A key limitation emerges when contrasting these real-world protocols with our simulation framework: actual evacuations are often delayed by the time required to initiate and propagate warnings, particularly when relying on less efficient communication channels. By contrast, our simulations assumed idealized conditions in which all pedestrian agents were already present on the street grid at the moment the evacuation alarm was triggered. Even under these optimal assumptions, our results revealed inefficiencies and delays in evacuation dynamics, inefficiencies that would likely be further amplified in real-world scenarios, where response times are slower and population movement less coordinated.

6. Conclusions

This paper presented a high-fidelity, agent-based evacuation study of Nicosia's Old Town, using a detailed 3D digital twin of the urban environment. The results demonstrate how legacy urban layouts amplify vulnerability and highlight the need for targeted infrastructural and procedural upgrades. Even under idealized conditions, assuming all agents are

already curbside when the alarm is triggered, most do not reach safety within the time frames recommended by civil protection guidelines. Furthermore, our experiments show that simply adding shelters without dynamic guidance can inadvertently increase congestion and travel times. Poor placement and lack of coordination often lead to chained rerouting and local bottlenecks. These findings underscore the importance of not only expanding capacity but also optimizing the spatial distribution of shelters and incorporating real-time decision support.

Limitations: While our digital twin captures detailed spatial and behavioral heterogeneity, several simplifications remain. First, all agents are assumed to start outdoors, omitting building egress delays. Additionally, both pedestrians and vehicles agents are modeled as homogeneous, lacking individualized decision-making or adaptive behavior in response to emergent threats. That is, agents do not exhibit realistic human responses under stress, such as fear, panic, urgency, or improvisation, nor do they vary in cognitive processing during emergencies. Instead, behavioral variation is introduced solely through differences in physical attributes, such as walking or driving speed. Moreover, the model does not incorporate probabilistic hazard layers (e.g., flood zones, earthquake risk) that could influence evacuation dynamics or route selection. Social dynamics, including group behavior, family units, or herding effects, are also not yet represented.

Future Work: We plan to address these limitations by introducing hazard overlays, crowd psychology modules, and individualized agent profiles based on local demographics and knowledge. Dynamic activation triggers (e.g., alarms or visual cues) will replace the assumption of simultaneous agent movement. Group-based behaviors, heterogeneous vehicle fleets, and integration with platforms like SUMO will further enhance realism. Ultimately, this work contributes a flexible simulation framework to support evidence-based planning for disaster resilience in historic urban areas.

Acknowledgments

The authors would like to thank the i-Nicosia project team for providing the 3D models of the old city of Nicosia as part of the digital twin concept.

References

Arrighi, C., Tanganelli, M., Cristofaro, M. T., Cardinali, V., Marra, A., Castelli, F., and De Stefano, M. (2023). Multi-risk assessment in a historical city. *Natural Hazards*, 119(2):1041–1072.

Batty, M. (2024). Digital twins in city planning. *Nature Computational Science*, 4(3):192–199.

Bernardini, G., Romano, G., Soldini, L., and Quagliarini, E. (2021). How urban layout and pedestrian evacuation behaviours can influence flood risk assessment in riverine historic built environments. *Sustainable Cities and Society*, 70:102876.

CYSTAT (2024). Census of population and housing 2021. Accessed: 2025.

Guy, S. J., Chhugani, J., Kim, C., Satish, N., Lin, M., Manocha, D., and Dubey, P. (2009). Clearpath: highly parallel collision avoidance for multi-agent simulation. In *Proceedings of the 2009 ACM SIGGRAPH/Eurographics Symposium on Computer Animation*, SCA '09, page 177–187, NY, USA. ACM.

Hassanpour, S. and Rassafi, A. A. (2021). Agent-based simulation for pedestrian evacuation behaviour using the affordance concept. *KSCE Journal of Civil Engineering*, 25(4):1433–1445.

Helbing, D., Farkas, I., and Vicsek, T. (2000). Simulating dynamical features of escape panic. *Nature*, 407(6803):487–490.

Kallmann, M. and Kapadia, M. (2014). Navigation meshes and real-time dynamic planning for virtual worlds. In *ACM SIGGRAPH 2014 Courses*, SIGGRAPH '14, NY, USA. ACM.

Kapadia, M., Beacco, A., Garcia, F., Reddy, V., Pelechano, N., and Badler, N. I. (2013). Multi-domain real-time planning in dynamic environments. In *Proceedings of the 12th ACM SIGGRAPH/Eurographics Symposium on Computer Animation*, SCA '13, page 115–124, NY, USA. ACM.

Karamouzas, I., Skinner, B., and Guy, S. J. (2014). Universal power law governing pedestrian interactions. *Phys. Rev. Lett.*, 113:238701.

Narain, R., Golas, A., Curtis, S., and Lin, M. C. (2009). Aggregate dynamics for dense crowd simulation. *ACM Trans. Graph.*, 28(5):1–8.

Pelechano, N., Allbeck, J. M., and Badler, N. I. (2007). Controlling individual agents in high-density crowd simulation. In *Proceedings of the 2007 ACM SIGGRAPH/Eurographics Symposium on Computer Animation*, SCA '07, page 99–108, Goslar, DEU. Eurographics Association.

Ronchi, E. and Nilsson, D. (2013). Fire evacuation in high-rise buildings: a review of human behaviour and modelling research. *Fire Science Reviews*, 2(1):7.

Therias, A. and Rafiee, A. (2023). City digital twins for urban resilience. *International Journal of Digital Earth*, 16(2):4164–4190.

van den Berg, J., Lin, M., and Manocha, D. (2008). Reciprocal velocity obstacles for real-time multi-agent navigation. In *Proceedings of the IEEE International Conference on Robotics and Automation*, pages 1928–1935.

Wang, Y., Yue, Q., Lu, X., Gu, D., Xu, Z., Tian, Y., and Zhang, S. (2024). Digital twin approach for enhancing urban resilience: A cycle between virtual space and the real world. *Resilient Cities & Struct.*, 3(2):34–45.

Yang, J., Zhan, H., Chen, L., and Dou, Z. (2022). Planning of emergency evacuation routes in densely populated urban areas during earthquakes. *Journal of Tsinghua University (Science and Technology)*, 62(1):70–76.

Zhang, X. and Chang, G.-l. (2014). A dynamic evacuation model for pedestrian–vehicle mixed-flow networks. *Transportation Research Part C: Emerging Technologies*, 40:75–92.

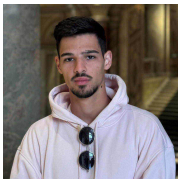

Marios Demetriou holds a BSc in Computer Science from the University of Cyprus. His interests lie at the intersection of computer graphics and large-scale, physics-based simulation, with a particular focus on modeling real-world environments and crowd dynamics.

Marios Stylianou holds a BSc in Computer Science from the University of Cyprus. His interests center on computer graphics and crowd dynamics, focusing on visually rich digital twins for large-scale evacuation simulation and urban resilience planning.

Andreas Aristidou is an Associate Professor in the Department of Computer Science at the University of Cyprus. He holds a PhD from the University of Cambridge, an MSc with honors from King's College London, and a BSc from the National and Kapodistrian University of Athens. His research focuses on computer graphics, with an emphasis on character animation. He employs machine learning and generative models to develop lifelike virtual humans.

A. Appendix

Table 1
Impact of Exit Closures on Average Evacuation Delay and Network Congestion.

Scenario	Avg. Addit. Evacuation Delay*	Main Impacts
Archbishop Makarios II Exit Closed	≈ 174 s (≈ 3 min)	Most severe impact. Large load shifts to Doros Loizou Bridge and Vasileos Georgiou B, causing extensive congestion on the peripheral road.
Vasileos Georgiou B Closed	≈ 149 s (≈ 2.5 min)	Second most severe. 56% of vehicles are redirected to Archbishop Makarios, significantly increasing congestion there.
Dorou Loizou Bridge Closed	≈ 146 s (≈ 2.3 min)	Similar impact to Vasileos Georgiou. Archbishop Makarios again absorbs the majority of the traffic flow.
Solomou Square Closed	≈ 53 s (≈ 1 min)	Minor impact. Paphos exit absorbs almost all redirected flow without saturation effects.
Paphos Closed	≈ 11 s	Negligible change. Low initial load, with easy redirection to Solomou Square exit.
Areos Street Closed (street, not exit)	≈ 55 s	Limited increase in time. Alternatives exist in the network, but local congestion appears on cross streets.

**Average difference at the 80%–90%–95% evacuation milestones compared to the pilot trial.*